NeuroImage 229 (2021) 117753

Contents lists available at ScienceDirect

NeuroImage

journal homepage: www.elsevier.com/locate/neuroimage

Children with attention-deficit/hyperactivity disorder spend more time in hyperconnected network states and less time in segregated network states as revealed by dynamic connectivity analysis

Heather M. Shappell[a,1,*], Kelly A. Duffy[b,2], Keri S. Rosch[c,d,e], James J. Pekar[f,g], Stewart H. Mostofsky[c,e,h], Martin A. Lindquist[a], Jessica R. Cohen[b,i,j]

[a] Department of Biostatistics, Bloomberg School of Public Health, Johns Hopkins University, Baltimore, MD, USA
[b] Department of Psychology and Neuroscience, University of North Carolina at Chapel Hill, Chapel Hill, NC, USA
[c] Center for Neurodevelopmental and Imaging Research, Kennedy Krieger Institute, Baltimore, MD, USA
[d] Department of Neuropsychology, Kennedy Krieger Institute, Baltimore, MD, USA
[e] Department of Psychiatry and Behavioral Sciences, Johns Hopkins University, Baltimore, MD, USA
[f] F.M. Kirby Research Center for Functional Brain Imaging, Kennedy Krieger Institute, Baltimore, MD, USA
[g] Department of Radiology and Radiological Science, Johns Hopkins University, Baltimore, MD, USA
[h] Department of Neurology, Johns Hopkins University, Baltimore, MD, USA
[i] Biomedical Research Imaging Center, University of North Carolina at Chapel Hill, Chapel Hill, NC, USA
[j] Carolina Institute for Developmental Disabilities, University of North Carolina at Chapel Hill, Chapel Hill, NC, USA

ARTICLE INFO

Keywords:
ADHD
Resting state
Dynamic functional connectivity
Hidden semi-Markov model
Default mode network
Task-relevant networks

ABSTRACT

Previous studies in children with attention-deficit/hyperactivity disorder (ADHD) have observed functional brain network disruption on a whole-brain level, as well as on a sub-network level, particularly as related to the default mode network, attention-related networks, and cognitive control-related networks. Given behavioral findings that children with ADHD have more difficulty sustaining attention and more extreme moment-to-moment fluctuations in behavior than typically developing (TD) children, recently developed methods to assess changes in connectivity over shorter time periods (i.e., "dynamic functional connectivity"), may provide unique insight into dysfunctional network organization in ADHD. Thus, we performed a dynamic functional connectivity (FC) analysis on resting state fMRI data from 38 children with ADHD and 79 TD children. We used Hidden semi-Markov models (HSMMs) to estimate six network states, as well as the most probable sequence of states for each participant. We quantified the dwell time, sojourn time, and transition probabilities across states. We found that children with ADHD spent less total time in, and switched more quickly out of, anticorrelated states involving the default mode network and task-relevant networks as compared to TD children. Moreover, children with ADHD spent more time in a hyperconnected state as compared to TD children. These results provide novel evidence that underlying dynamics may drive the differences in static FC patterns that have been observed in ADHD and imply that disrupted FC dynamics may be a mechanism underlying the behavioral symptoms and cognitive deficits commonly observed in children with ADHD.

1. Introduction

Attention-deficit/hyperactivity disorder (ADHD) is characterized by developmentally inappropriate symptoms of inattention, impulsivity, and hyperactivity. These symptoms are thought to be driven by atypical brain network organization and dysfunctional connectivity (Cao et al., 2014; Henry and Cohen, 2019). Research investigating disrupted functional connectivity (FC) in ADHD, often during a resting state (Castellanos and Aoki, 2016), has focused primarily on estimating average FC over the course of an experimental scanning session, sometimes referred to as "static" FC. However, recently there has been growing interest in studying changes in connectivity over shorter time periods (i.e., "dynamic" FC), for example on the second-to-minute scale (Calhoun et al., 2014; Hutchison et al., 2013; Lurie et al., 2020). Given that the brain is a dynamic system, it is believed that individuals transition in and out of multiple brain states during the course of a

* Correspondence to: Heather Shappell, 525 Vine Street, Winston-Salem, NC 27157-1063, United States.
E-mail address: hshappel@wakehealth.edu (H.M. Shappell).
[1] Heather Shappell is now with the Department of Biostatistics and Data Science, Wake Forest School of Medicine, Winston Salem, NC, USA.
[2] Kelly Duffy is now with the Department of Psychology, University of Minnesota, Minneapolis, MN, USA.

https://doi.org/10.1016/j.neuroimage.2021.117753
Received 11 November 2020; Received in revised form 17 December 2020; Accepted 6 January 2021
Available online 14 January 2021

single scanning session. Thus, there is a need to investigate how these dynamics relate to behavior and disease (Calhoun et al., 2014; Cohen, 2018; Kucyi et al., 2018). Investigating dynamic FC may be particularly relevant for understanding the neurobiological basis of ADHD given that behavioral variability is a ubiquitous finding in the neurocognitive and clinical literature (Castellanos et al., 2009; 2005; Karalunas et al., 2014; Kofler et al., 2013). Indeed, studies probing dynamic FC in ADHD are beginning to emerge and support the proposal that dynamic FC is a useful tool for understanding the neural underpinnings of ADHD (Abbas et al., 2019; Cai et al., 2018; de Lacy and Calhoun, 2019; Kaboodvand et al., 2020; Wang et al., 2018).

Previous studies in ADHD applying static FC analyses have observed network disruption both on a whole-brain, global connectivity scale, in which high-level organizational differences in how the brain functions are observed in ADHD as compared to in control participants, as well as on a sub-network scale, in which individual, well-known networks are affected by the disorder (Cao et al., 2014; Castellanos and Proal, 2012). Specifically, it has been reported that individuals with ADHD show atypical small-world architecture characterized by higher local efficiency combined with lower global efficiency (Lin et al., 2014; Wang et al., 2009). Further, sub-networks such as the default mode, salience, attention, cognitive control, and motor networks are thought to be particularly affected by ADHD (Castellanos and Aoki, 2016). For example, altered within-default mode network (DMN) FC (Fair et al., 2010; Kessler et al., 2014; Sripada et al., 2014; Sun et al., 2012) and decreased magnitude of negative correlations between DMN and regions of task-relevant networks, including those related to attention and cognitive control (Kessler et al., 2014; Mills et al., 2018; Sripada et al., 2014; Sun et al., 2012), have been repeatedly reported in ADHD. However, despite these generally consistent findings, some recent literature has not observed static FC differences between the DMN and task-relevant networks in ADHD, particularly networks related to cognitive control (Dajani et al., 2019; de Lacy and Calhoun, 2019). Further, three recent meta-analyses examining static FC alterations in ADHD have been conducted with inconsistent results. Specifically, while two report differences within and between DMN and task-relevant network FC in individuals with ADHD as compared to control participants (Gao et al., 2019; Sutcubasi et al., 2020), a third observes no brain regions with significant FC alterations in ADHD (Cortese et al., 2020). These recent findings imply that static FC may not be the most appropriate biomarker to differentiate ADHD from TD individuals.

Given promising recent findings of studies that have investigated dynamic FC, in combination with the potential limitations of static FC, dynamic FC may be a particularly useful technique for gaining insight into dysfunctional FC in ADHD, especially since moment-to-moment fluctuations in behavior are greater in children with ADHD than in typically developing (TD) children. Reaction time (RT) variability is higher in ADHD (Karalunas et al., 2014; Kofler et al., 2013), and periodic fluctuations in RT across time are stronger in children with ADHD than in TD children (Castellanos et al., 2005; Di Martino et al., 2008; Karalunas et al., 2013; Vaurio et al., 2009). Notably, the frequency range in which these RTs oscillate (.02–.07 Hz) is similar to the range of low frequency BOLD oscillations that can be detected with resting state FC. Most relevant to this are DMN fluctuations, as it is thought that DMN intrusions into task-relevant processing underlie lapses of attention (Sonuga-Barke and Castellanos, 2007; Weissman et al., 2006). The small body of literature probing dynamic FC in ADHD has indeed supported the importance of the DMN, although the observed role of DMN dynamics in ADHD is not entirely consistent. Some literature has found that dynamics as related to the DMN are restricted, including within the DMN (de Lacy and Calhoun, 2019), between the DMN and a task-positive network (Abbas et al., 2019), and between the DMN and sensory networks (the auditory network in particular) (Wang et al., 2018). Conversely, other literature has reported that more variable FC between the DMN and task-relevant networks is observed in ADHD (Cai et al., 2018; Kaboodvand et al., 2020). Notably, using a machine learning approach, it has been found that when equating the number of features going into the model, dynamic FC is better at discriminating between ADHD and TD participants than conventional measures of static FC (Wang et al., 2018). Moreover, as further support that DMN-related dynamic FC is relevant to ADHD, it has been observed that more variable interaction patterns between the DMN and task-relevant networks are correlated with ADHD symptomatology (both inattention and hyperactivity/impulsivity) (Cai et al., 2018) and that stability of FC patterns within the DMN and between the DMN and task-relevant cognitive control networks are related to cognitive control performance, as operationalized by Stroop task incongruent reaction times in adults with and without ADHD (Kaboodvand et al., 2020).

The above suggests that dynamic FC analysis holds promise to identify mechanisms and characteristics contributing to the ADHD phenotype. Hidden semi-Markov models (HSMMs) may help to resolve the inconsistent findings in the literature because they produce more accurate estimates of state traversal compared to other common dynamic FC analysis methods, such as sliding window and standard hidden Markov models (HMMs). More specifically, HSMMs have the benefits of standard HMMs, including the ability to handle large amounts of data and the capability to detect rapid changes in dynamic FC, but they additionally have the major advantage of explicitly modeling and estimating sojourn distributions (the amount of time spent in each state before switching to another) (Shappell et al., 2019).

Therefore, we utilized HSMMs to assess transitions across distinct FC states in children with ADHD and TD children. We quantified each participant's most probable sequence of network states, along with time spent in each state, sojourn distributions, and probabilities of transitioning across states. We hypothesized that sojourn distributions would be particularly discriminative across groups, implying that children with ADHD may have trouble traversing in and out of certain states. Specifically, we predicted that children with ADHD may get 'stuck' in an inattentive state characterized by high connectivity between the DMN and task-relevant networks, while they would be less likely to enter into or maintain a cognitive control, or on-task attention, state characterized by anticorrelations between the DMN and task-relevant networks.

2. Materials and methods

2.1. Participants

Participants in this study included 38 participants with ADHD (mean age 10.21 years, 9 females) and 79 TD participants (mean age 10.23 years, 25 females) between 8 and 13 years. Groups were matched for age, sex, IQ, and socioeconomic status. Participants were a subset of those from a larger study and selected if they had sufficient good quality resting state data (see *Data and processing* for details). Importantly, when comparing demographic and clinical characteristics of the included and excluded participants with ADHD, we found that the groups did not differ in terms of age, sex, socioeconomic status, IQ, ADHD symptomatology (inattention or hyperactivity), number of participants with comorbid disorders, number of participants on stimulant medication, or number of participants on medication to treat comorbidities (selective serotonin reuptake inhibitors or other psychotropic drugs; all p-values > 0.24, false discovery rate [FDR]-corrected for 10 comparisons). Similarly, included and excluded TD participants did not differ in terms of age, sex, socioeconomic status, IQ, or ADHD symptomatology (inattention or hyperactivity; all p-values > 0.87, false discovery rate [FDR]-corrected for 6 comparisons; TD participants were not enrolled in the study if they had comorbidities or were taking ADHD or other psychotropic medication). Thus, our sample of included participants was representative of the larger sample from which they were pulled.

Both ADHD and TD participants were primarily recruited through local public schools, with additional resources including community-wide advertisements, volunteer organizations, medical institutions, and word

Table 1
Demographic information and clinical characteristics. Results are presented as Mean (SD) or N (%) unless otherwise stated. FD = framewise displacement. GAI = General Ability Index on the WISC-IV or WISC-V (Wechsler, 2003b; 2014), which was our measure of IQ. SES = socioeconomic status of parents (Hollingshead, 1975). †T-scores from Conners Parent Rating Scales-Revised or Conners-3 (Conners, 2002; 2008). * = significant group difference two-sample t-tests (or, in the case of sex and comorbid diagnoses, two-sample chi-squared tests), FDR-corrected $p < .05$.

	ADHD (n = 38)	TD (n = 79)	P-value (corrected)
Age (yrs)	10.21 (1.24)	10.23 (1.04)	0.93
Sex (M/F)	29 / 9	54 / 25	0.45
SES	54.74 (7.43)	54.51 (8.71)	0.93
GAI	113.21 (15.50)	117.92 (12.86)	0.15
Oppositional defiant disorder diagnosis	15 (39.47%)	0 (0%)	0.00*
Conduct disorder diagnosis	1 (2.6%)	0 (0%)	0.20
Depression diagnosis	1 (2.6%)	0 (0%)	0.20
Anxiety diagnosis	2 (5.3%)	0 (0%)	0.08
Specific phobia diagnosis	6 (15.8%)	1 (1.3%)	0.005*
ADHD Inattentive T-Score†	74.18 (9.52)	45.47 (5.54)	1.4E-39*
ADHD Hyperactive T-Score†	71.45 (15.14)	46.44 (5.19)	3.5E-24*
Currently taking stimulant medication	24 (65.8%)	N/A	N/A
Naïve to stimulant medication	10 (26.3%)	N/A	N/A
Taking other psychotropic medication	3 (7.9%)	N/A	N/A
Motion during resting state scan: FD (mm)	0.15 (0.06)	0.12 (0.04)	0.001*

of mouth. This study was approved by the Johns Hopkins Institutional Review Board. After complete description of the study to each participant and a parent or guardian, written informed consent was obtained from the parent/guardian, and assent was obtained from the child.

Participants received an ADHD diagnosis if they met criteria for ADHD using either the Diagnostic Interview for Children and Adolescents, Fourth Edition (Reich et al., 1997) or the Kiddie Schedule for Affective Disorders and Schizophrenia for School-Aged Children-Present and Lifetime Version (Kaufman et al., 1997), in addition to either 1) a t-score ≥ 60 on the Inattentive or Hyperactive subscales of the Conners' Parent or Teacher Rating Scales-Revised Long Version or the Conners-3 (Conners, 2002; 2008), or 2) a score of ≥ 2 on at least 6 items on the Inattentive or Hyperactivity/Impulsivity scales of the ADHD Rating Scale-IV, Home or School Versions (DuPaul et al., 1998). Inclusion in the TD group required scores below clinical cut-offs on the parent and teacher (when available) Conners' and ADHD Rating Scales, as well as no immediate family members diagnosed with ADHD. Additional inclusion criteria was as follows: no history of intellectual disability, seizures, traumatic brain injury or other neurological illness; no history of psychosis, autism spectrum disorder, or reading disorder for ADHD participants (for TD participants, no history of any psychiatric or developmental disorder other than specific phobia); no current psychoactive medication (TD participants only; short-acting stimulant medication to treat ADHD, as well as other medication to treat comorbidities, was OK for ADHD participants; participants on other ADHD medications were excluded); no MRI contraindications; full scale intelligence quotient (FSIQ) ≥ 80 as assessed with the Wechsler Intelligence Scale for Children, Fourth or Fifth Edition (WISC-IV or WISC-V) (Wechsler, 2003b; 2014), and Word Reading score from the Wechsler Individual Achievement Test, Second or Third Edition (Wechsler, 2003a; 2009) ≥ 85. Comorbidities in the ADHD group included: oppositional defiant disorder (15), conduct disorder (1), unspecified depressive disorder (1), anxiety disorders, including generalized anxiety disorder and separation anxiety (2), and specific phobia (6). Children with ADHD on short-acting stimulant medication (6 girls, 19 boys) were eligible to participate if they withheld medication the day prior to and day of testing. Three participants were taking longer-acting psychoactive medication and were not asked to withhold that medication before testing (all three were taking a selective serotonin reuptake inhibitor; one was additionally taking an antipsychotic). Participant demographics and clinical characteristics are summarized in Table 1.

2.2. Data and processing

Resting state functional MRI data was collected at the Kennedy Krieger Institute F. M. Kirby Research Center for Functional Brain Imaging using a 3-Tesla Philips Achieva whole-body MR machine. Data were collected using either an 8-channel head coil (n = 59) or a 32-channel head coil (n = 67; n = 5 not recorded). Whole-brain functional data were acquired using a multi-slice SENSE-EPI pulse sequence (TR = 2500 ms, TE = 30 ms, SENSE factor = 2, flip angle = 70°, 47 contiguous ascending 3 mm slices with in-plane resolution of 3.05 mm × 3.15 mm). Participants were instructed to stay awake with their eyes open and to fixate on a white crosshair in the center of a gray screen. Participants received a single resting state run that lasted either 5.3 min (128 timepoints; n = 11) or 6.5 min (156 timepoints; n = 120). A high-resolution T1-weighted (T1w) structural 3D MP-RAGE was also acquired (TR = 8 ms, TE = 3.7 ms, flip angle = 8°, resolution = 1 mm × 1 mm × 1 mm).

Functional data were minimally preprocessed using FMRIPREP version 1.0.7 (Esteban et al., 2019), a Nipype (Gorgolewski et al., 2011; 2017) based tool. Each T1w volume was corrected for INU (intensity non-uniformity) using N4BiasFieldCorrection v2.1.0 (Tustison et al., 2010) and skull-stripped using antsBrainExtraction v2.1.0 (using the OASIS template). Brain surfaces were reconstructed using recon-all (FreeSurfer v6.0.0) (Dale et al., 1999). The brain mask estimated previously was refined with a custom variation of the method to reconcile ANTs-derived and FreeSurfer-derived segmentations of the cortical gray-matter of Mindboggle (Klein et al., 2017). Spatial normalization to the ICBM 152 Nonlinear Asymmetrical template version 2009c (Fonov et al., 2009) was performed through nonlinear registration with antsRegistration (ANTs v2.1.0) (Avants et al., 2008), using brain-extracted versions of both T1w volume and template. Brain tissue segmentation of cerebrospinal fluid (CSF), white-matter (WM) and gray-matter (GM) was performed on the brain-extracted T1w using fast (FSL v5.0.9) (Zhang et al., 2001).

Functional data was slice time corrected using 3dTshift (AFNI v16.2.07) (Cox, 1996) and motion corrected using mcflirt (FSL v5.0.9) (Jenkinson et al., 2002). This was followed by co-registration to the corresponding T1w using boundary-based registration (Greve and Fischl, 2009) with 9° of freedom, using bbregister (FreeSurfer v6.0.0). Motion correcting transformations, BOLD-to-T1w transformation and T1w-to-template (MNI) warp were concatenated and applied in a single step using antsApplyTransforms (ANTs v2.1.0) using Lanczos interpolation.

Physiological noise regressors were extracted from mean signal within CSF and WM. Framewise displacement (FD) (Power et al., 2014) was calculated for each functional run using the implementation of Nipype.

Many internal operations of FMRIPREP use Nilearn (Abraham et al., 2014), principally within the BOLD-processing workflow. For more details of the pipeline see http://www.fmriprep.readthedocs.io/en/latest/workflows.html.

Following the minimal preprocessing, data were bandpass filtered (.01–0.8 Hz), and 32-parameter nuisance regression was applied (6 rigid body motion parameters, mean CSF and mean WM; temporal derivatives and quadratic expansions of these 8 regressors; quadratic expansions of the 8 temporal derivatives). We chose this processing stream following recommendations from Ciric and colleagues (Ciric et al., 2017) and Parkes and colleagues (Parkes et al., 2018). Participants were included in this sample if they had mean FD < 0.28mm and no individual spikes in motion > 0.75mm. Mean FD was larger for the participants with ADHD than for the TD participants (mean ADHD: 0.153mm; mean TD: 0.117mm; $t(129) = 4.11$, $p < .0001$). We chose to not match the groups on mean FD given evidence that head motion is correlated with ADHD symptomatology and that head motion and ADHD may have similar genetic loadings (Couvy-Duchesne et al., 2016). Thus, matching groups on mean FD could result in a non-representative sample of children with ADHD. To ensure that our data processing sufficiently removed motion-related artifacts from the data in both groups of participants, we calculated motion-related quality control metrics on the postprocessed data (Ciric et al., 2017) and correlated mean FD across participants with our output metrics from the HSMM: dwell times and mean/maximum sojourn times (see *Statistical inference and permutation testing* for description of the metrics). We further assessed whether any of the states were related to high motion timepoints by comparing the mean FD for timepoints within each state to that of the other states. See *Supplementary Material* for description of our motion-related quality assurance steps and findings.

Following processing, we partitioned the brain into 100 cortical ROIs using the functional Local-Global Atlas (Schaefer et al., 2018). We focused our investigation on networks found to be dysfunctional in ADHD (Cao et al., 2014; Castellanos and Proal, 2012; Henry and Cohen, 2019), resulting in a subset of 70 ROIs. We used the 17-network parcellation from Yeo and colleagues (Yeo et al., 2011) to define the network to which each ROI was assigned. These included the default mode network (DMN; Default A/B/C: 21 regions), fronto-parietal control network (FP; Control A/B/C: 16 regions), salience/ventral attention network (SAL/VAN; Salience/VenAttn A/B: 14 regions), dorsal attention network (DAN; Dorsal Attention A/B: 13 regions), and hand somatomotor network (SM; Somatomotor A: 6 regions). The fully processed time-series data were averaged within each ROI, and these ROI time-series were used in analyses.

2.3. Hidden semi-Markov modeling

We implemented an HSMM on our entire data set. For results implementing separate models for the ADHD and TD groups, see *Supplementary Material*. We denote the ROI time-series data for each participant by $Y_{i1}, ..., Y_{iT}$, where each $p-$dimensional vector Y_{it} contains the BOLD measurements of the p ROIs at the t^{th} timepoint for the i^{th} participant. The collection of vectors of observed time-series data is denoted by $\tilde{Y}_i$. We represent a true/hidden network index variable underlying the observed time-series vectors at a particular observation time by S_{it}. The vector of true network state variables, $S_{i1}, ..., S_{iT}$, is denoted by $\tilde{S}_i$.

We assume that each Y_{it} follows a multivariate Gaussian distribution $Y_{it} \sim \mathcal{N}(\mu_{s=k}, \Sigma_{s=k})$, in which the mean and covariance are dependent on the current (unknown) network state k of the timepoint. Thus, each network state has its own set of mean activations across our pre-specified ROIs, as well as its own covariance/correlation structure between ROIs. For our main analysis, we fit one set of network states using the data across all individuals (see *Supplementary Material* for states fit on ADHD and TD individuals separately). The number of states one can fit must be specified a-priori and is heavily dependent on the number of participants, number of timepoints, and number of ROIs. This is because as the number of states increases, the number of parameters required to be estimated similarly increases. Given our sample size, we found that six states produced stable parameter estimates over multiple fittings of the model.

We used the HSMM, an extension of the standard HMM, to model our data (Fig. 1) (Shappell et al., 2019). The main difference is that the sojourn time distribution is explicitly defined in the HSMM, and therefore is able to be estimated. Each underlying brain state variable is dependent on two items – the previous network state and the amount of time spent in the current network state. These two items are modeled by transition probabilities and sojourn time distributions. In this paper, we used a smoothed-nonparametric sojourn distribution since we do not know the exact form of the sojourn distribution. See *Supplementary Material* for the complete data log-likelihood of the HSMM.

2.4. Maximum likelihood estimation

The HSMM parameters (mean vector and covariance matrix for each state, initial state probabilities, sojourn distributions, and state transition probabilities) were estimated utilizing the *mhsmm* R package (O'Connell et al., 2011). This package allows for inference for multiple observation sequences (i.e., multiple participants at once). Therefore, we concatenated each individual's time-series data so that the total number of rows in our data set was equal to the sum of the time-series lengths across all individuals. The number of columns in our data set was equal to the number of ROIs ($n = 70$). The HSMM parameters were then estimated on this entire data set, resulting in one set of model parameter estimates. Results showing estimates obtained from fitting the model on TD and ADHD groups separately are presented in the *Supplementary Material*.

The Expectation-Maximization algorithm (Dempster et al., 1977) was used to estimate all model parameters. Each participant's most probable sequence of true network states was estimated using the Viterbi Algorithm (Forney, 1973). The Viterbi algorithm takes the state estimates, transition probability estimates, sojourn density estimates, and initial state probability estimates obtained from fitting the HSMM on all participants and calculates each individual participant's most likely sequence of states given those estimates, along with the participant's BOLD time-series data. In other words, the Viterbi algorithm takes an individual's time-series data and finds which of the six states estimated from the entire data set that the data is suggesting he/she is in at each timepoint. Therefore, although the state estimates are based on the entire data set and are not subject-specific, when a state is active is subject-specific. A further description of the model estimation procedure, including how the non-parametric sojourn densities were estimated, can be found in Shappell et al. (2019).

2.5. State graph metric calculation

To better characterize each of the states, graph metrics of network organization were calculated. Correlation matrices obtained from each of the six fitted states were used to construct undirected, weighted graphs. All negative correlation values were set to 0. The Brain Connectivity Toolbox (www.brain-connectivity-toolbox.net) (Rubinov and Sporns, 2010) was then used to calculate global efficiency, local efficiency, and modularity for each state.

Global efficiency is defined as the inverse of the average shortest path length in the network (Latora and Marchiori, 2001) and is a measure of overall network integration, which can be conceived of as how quickly information can pass across an entire network. Local efficiency for a given node is defined as the average inverse shortest path length among neighboring nodes of that node (i.e., those directly connected

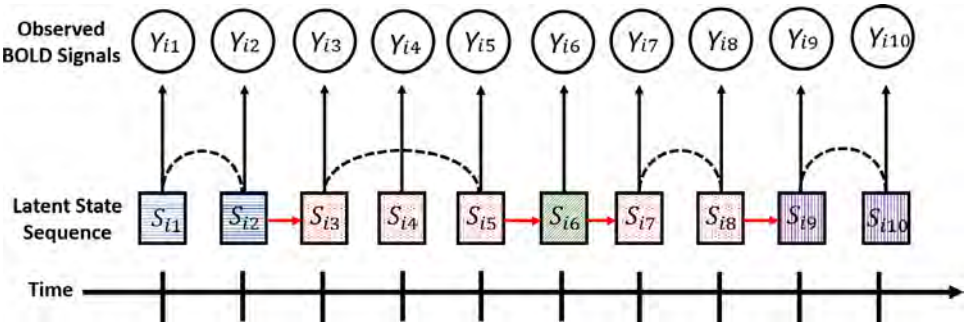

Fig. 1. Hidden semi-Markov model overview. The unobserved hidden states evolve according to a semi-Markov process characterized by state transition probabilities (underlying the red arrows) and duration densities/sojourn distributions (dashed lines). The BOLD signals at each timepoint are assumed to follow a Gaussian distribution with parameters that depend on the current network state.

to the node of interest) (Latora and Marchiori, 2001). Local efficiency is a measure of the efficiency of information transfer within a network of neighboring (i.e., local) nodes. Modularity quantifies the degree of segregation of a network into distinct subnetworks by relating the number of within-network connections to all connections, such that higher values indicate a greater degree of segregation (Newman, 2004). For equations of these calculated graph metrics, see *Supplementary Material*.

2.6. Statistical inference and permutation testing

We assessed the relationship between ADHD diagnosis and dwell times and empirical sojourn distributions of the brain states inferred from the HSMM. A participant's dwell time for each state was calculated by summing the total number of timepoints spent in that state and dividing by the length of the participant's time-series, then converting to a percent. Group averages were then calculated for each state by finding the mean across all participants in each group. To calculate the empirical sojourn distribution of each state for a participant, we counted the number of consecutive timepoints the participant remained in a given state. We then gathered these counts across all participants in each group and computed a density estimate for each group from the counts. For all calculations involving sojourn times, we left out the starting state sequence and ending state sequence for every individual. We did this to avoid a bias towards shorter sojourn times since we had no way of knowing how long the individual was in the state before beginning the scan or after ending the scan.

After obtaining separate empirical sojourn distributions for each group for all 6 states, we performed a group comparison of each state's empirical sojourn distribution using Kullback-Leibler (KL) divergence, a measure of the directed divergence between two probability distributions. See Shappell et al. (2019) for a more detailed description of the KL divergence in this context. In the simple case, a KL divergence of 0 indicates identical behavior from both distributions, whereas a KL divergence of 1 indicates vastly different behavior. The *Philentropy* R package was used to calculate the KL divergence.

To determine if any observed dwell time and/or sojourn distribution differences were statistically significant, we performed a permutation test based on 500 permuted samples.

2.7. Relationships with ADHD symptoms

Finally, we examined whether dwell times or sojourn distributions of the derived states were related to symptoms in the participants with ADHD. To do so, we extracted dwell time and sojourn time for each participant with ADHD and correlated those metrics with symptom severity as assessed using *t*-scores on the Conners' Parent Rating Scale, both for the Inattentive and Hyperactive subscales. We could not reliably estimate the entire sojourn distribution on an individual participant level given the small sample size (i.e., we would need a much longer scan or multiple scans for each individual), so instead we extracted mean and maximum sojourn time associated with each state for each participant with ADHD. We focused our analyses on states and HSMM metrics that showed group differences and used the FDR correction for the appropriate number of comparisons.

3. Results

3.1. Functional brain state characterization

First, we investigated the FC patterns of the six network states estimated using the HSMM (Fig. 2). State 6 differed substantially from the other states with regard to FC patterns, with globally stronger positive correlation values and no negative correlations. The average positive correlation value between the ROIs in state 6 was 0.44, as compared to 0.24, 0.31, 0.26, 0.25, and 0.29 in states 1, 2, 3, 4, and 5, respectively.

In contrast, states 1–5 all consisted of negative correlations between the DMN and other networks, with states 1, 3, and 4 having the greatest number of negative correlations (282, 101, and 144 compared to 25, 61, and 0 in states 2, 5, and 6). In particular, states 1, 3, and 4 had more negative correlations between the DMN and SAL/VAN compared to states 2, 5, and 6 (110, 60, and 83 compared to 22, 44, and 0 in states 2, 5, and 6). Additionally, states 1 and 4 had more negative correlations between the DMN and DAN compared to the other states (104 and 34 versus 2, 10, 5, and 0 in states 2, 3, 5, and 6).

Fig. 3 presents the connectivity differences between states 1, 3, and 4 (the three states containing the largest number of negative correlations) by showing a heat map of the difference in correlation values for all pairs of regions between state 3 and states 1 and 4. We choose state 3 as the common comparison state for the figure because it differed in both dwell time and sojourn distribution between the two diagnostic groups (see Results sections *State dwell times* and *State sojourn times*, as well as Figs. 7 and 8). Overall, state 1 had stronger negative correlations as compared to states 3 and 4, with an average negative correlation value of 0.076 (states 3 and 4 had averages of 0.061 and 0.072, respectively). Moreover, state 1 had a greater number of stronger negative correlation values between SAL/VAN and DMN ROI pairs compared to states 3 and 4 (68% of the top 25% strongest negative correlation values came from state 1, while 28% came from state 3 and 4% came from state 4).

Additionally, state 3 had stronger positive correlations within and between the SM and DAN as compared to states 1 and 4. Positive within SM ROI pairs had a mean correlation value of 0.623 for state 3 versus 0.521 and 0.518 for states 1 and 4, respectively. Positive within DAN ROI pairs had a mean correlation value of 0.491 for state 3 compared to 0.433 and 0.440 for states 1 and 4. Moreover, positive between SM-DAN correlations had a mean value of 0.399 for state 3 compared to 0.340 and 0.336 for states 1 and 4. Therefore, state 1 had the strongest negative correlations between the SAL/VAN and DMN, while state 3 (which had the second strongest number of negative correlations) had the strongest positive correlations within and between task-relevant networks (i.e., SM and DAN). States 1 and 3 are two states we would expect to observe when someone is in an attentive, externally-oriented state.

In addition to connectivity differences, the activation patterns of the six states differed. Most notably, state 6 had above average activation levels. The average positive z-scored activation value in state 6 was

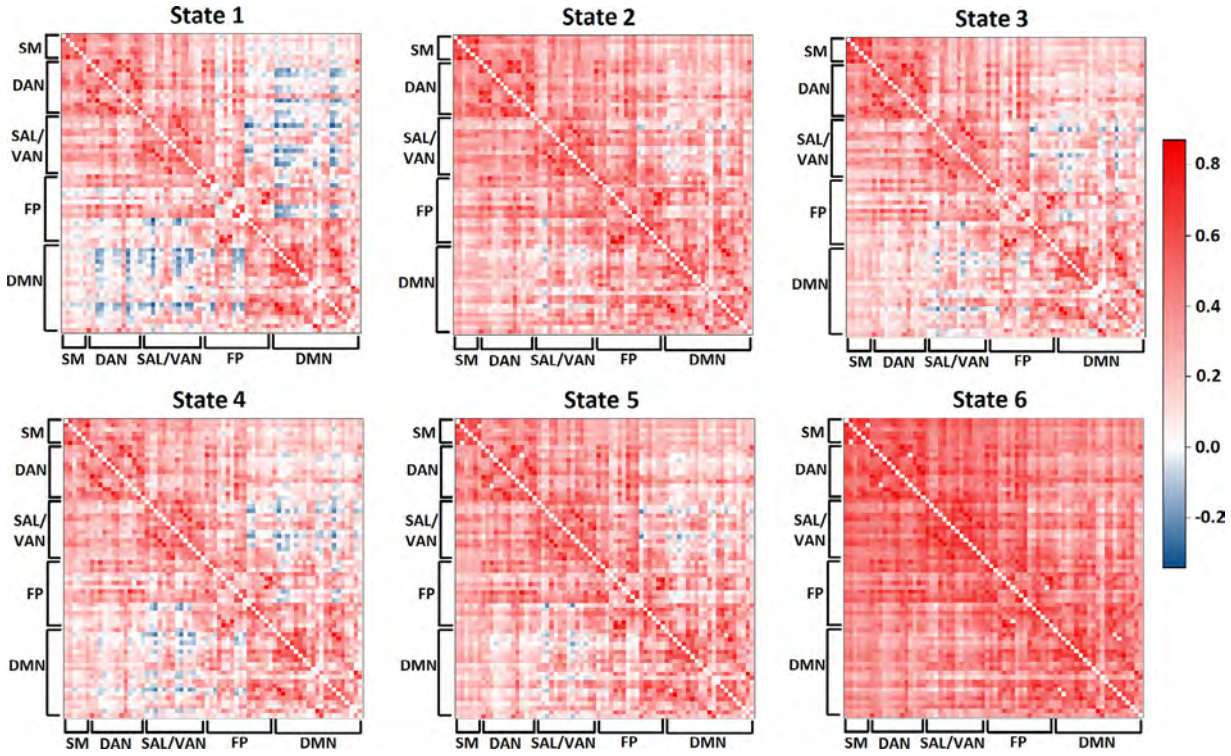

Fig. 2. Pearson correlation matrices for the six states estimated via the HSMM. These six states represent the functional connectivity patterns that occurred in all participants regardless of group during the resting state scan. Red cells indicate a positive correlation between the two corresponding ROIs, while blue cells indicate a negative correlation (or anticorrelation). Individual ROIs are grouped by intrinsic network. These include the default mode network (DMN; Default A/B/C: 21 ROIs), fronto-parietal control network (FP; Control A/B/C: 16 ROIs), salience/ventral attention network (SAL/VAN; Salience/VenAttn A/B: 14 ROIs), dorsal attention network (DAN; Dorsal Attention A/B: 13 ROIs), and hand somatomotor network (SM; Somatomotor A: 6 ROIs).

Table 2
Metrics derived from graph theory that quantify whole-brain topology for each of the 6 states.

	State 1	State 2	State 3	State 4	State 5	State 6
Global Efficiency	0.2661	0.3290	0.2888	0.2782	0.3219	0.4457
Local Efficiency	0.2214	0.2932	0.2425	0.2287	0.2780	0.4307
Modularity	0.2380	0.0826	0.1521	0.1636	0.1074	0.0316

0.024 compared to 0.013, 0.009, 0.017, 0.019, and 0.014 in states 1–5, respectively. Of the other five states, states 1 and 5 stood out as having below average activation values across a majority of the resting-state sub-networks compared to states 2–4 (average negative z-scored values of 0.024 and 0.030 for states 1 and 5 versus 0.014, 0.016, and 0.013 for states 2, 3, and 4). States 2–4 had a mix of above average activation values and below average activation values across the 70 ROIs (Fig. 4)

3.2. Topological characteristics of the brain states

To further characterize the brain states, we quantified aspects of global topology of each of the states. Table 2 presents the global efficiency, local efficiency, and modularity of each of the 6 states. Fig. 5 reveals the topology of the top 20% of positive correlations for all six states (taking into account the connections over all six states, as opposed to each state individually).

State 6 had the highest global and local efficiency and lowest modularity of all six states. As is evident in the graphical representation (Fig. 5), state 6 consisted of stronger positive correlation values than any other state, and the nodes of different sub-networks were less separated than for the other states. These observations support the conclusion that state 6 was hyperconnected both within and across sub-networks. The low value of modularity further indicates that all sub-networks were strongly connected to each other, meaning there was not a strong bias for segregation across sub-networks.

States 2 and 5 had somewhat high values of global and local efficiency compared to states 1, 3, and 4, although all values were more moderate than state 6. States 2 and 5 additionally had lower relative values of modularity. This is also reflected in the graphical representation of these states (Fig. 5), as states 2 and 5 contained more connections and less segregation across sub-networks than states 1, 3, and 4.

In terms of global topology, states 1, 3, and 4 were similar, with relatively low values of global and local efficiency and relatively high values of modularity. As described above, the strength of connections differentiated these states from each other more so than overall topology. Specifically, state 1 consisted of stronger negative correlations between the DMN and the SAL/VAN compared to states 3 and 4, while state 3 had the strongest positive correlations within and between the SM and DAN.

3.3. State dwell times

We predicted the most likely state sequence for each participant (Fig. 6). Of interest was the total percentage of estimated time participants spent in each state (dwell time) during the course of their resting state scan. Numerically, children with ADHD spent a larger percentage

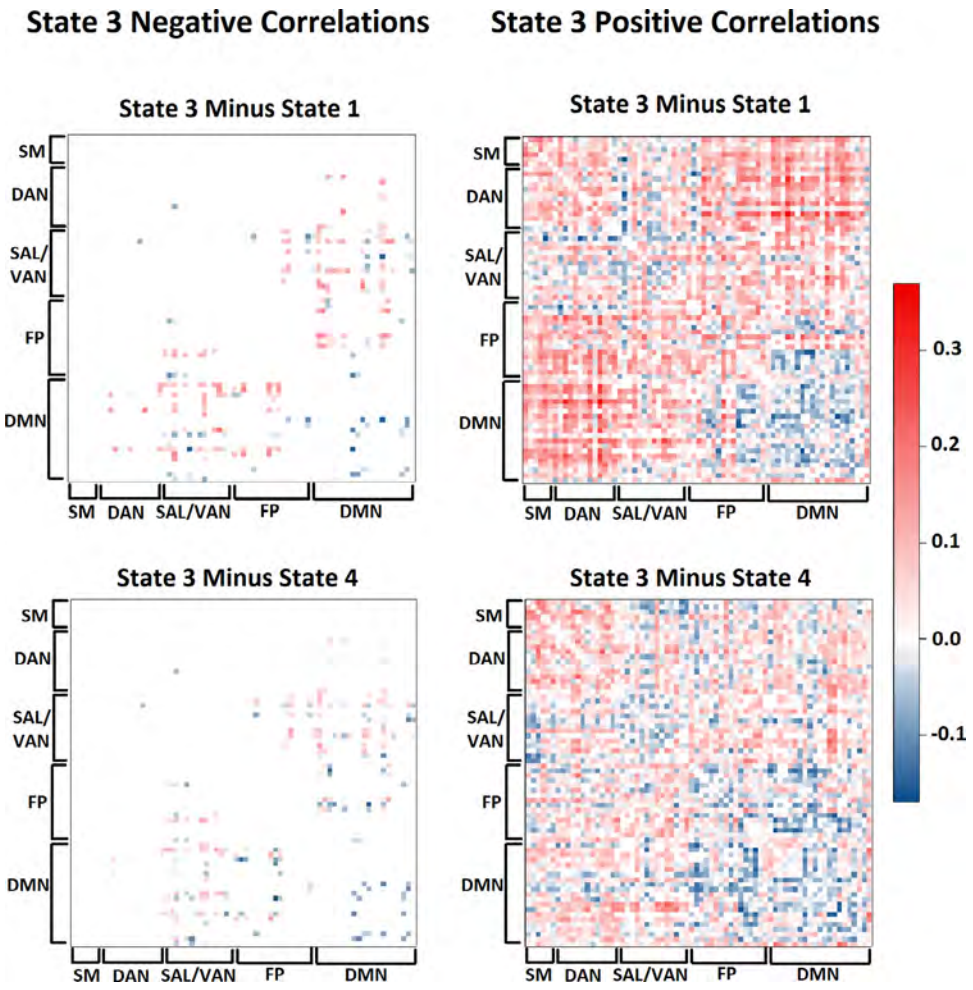

Fig. 3. Differences in correlation values between state 3 and states 1 and 4. Left column: The correlation differences for the subset of ROI pairs that had a negative correlation for state 3 (solid white cells represent ROI pairs not in this subset or ROI pairs that have no difference between the two states). Blue cells indicate either a weaker negative or a positive correlation as compared to state 3. Red cells represent pairs of ROIs in which the correlation was more strongly negative as compared to state 3. Right column: The correlation differences for the subset of ROI pairs that had a positive correlation for state 3 (again, solid white cells represent ROI pairs not in this subset or ROI pairs that have no difference between the two states). Blue cells indicate a stronger positive correlation as compared to state 3. Red cells indicate a negative correlation or a weaker positive correlation as compared to state 3.

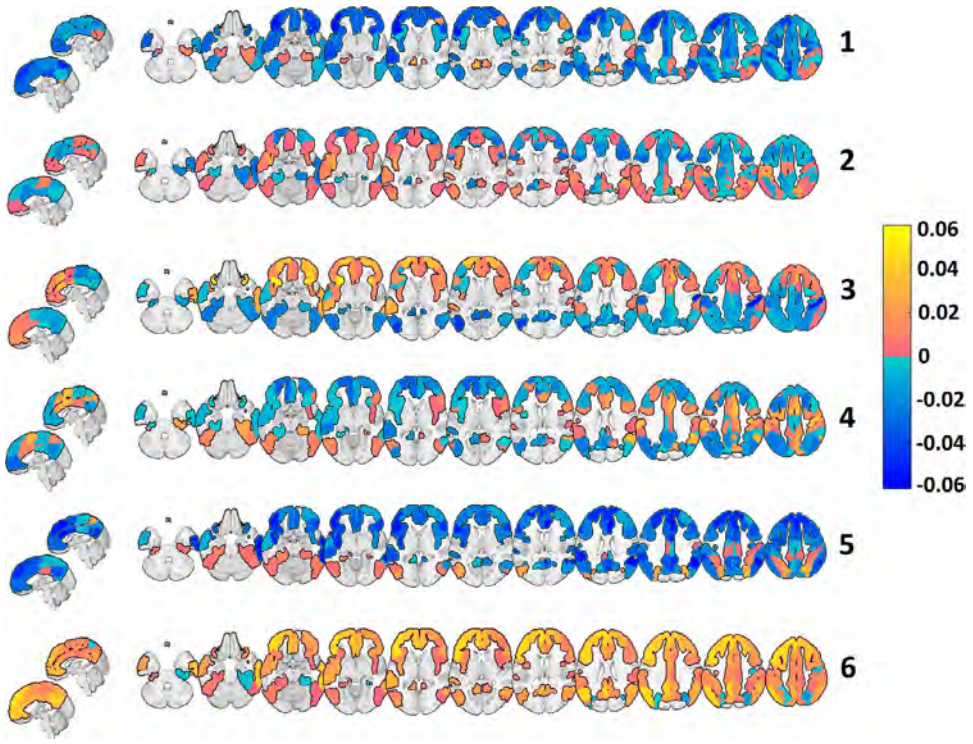

Fig. 4. Mean z-scored activation levels estimated via the HSMM, as described in Section 2.3, for each ROI across the six estimated brain states. Red, orange, and yellow areas indicate regions that have above average activation levels for a particular state, while green and blue areas indicate regions with below average activation levels.

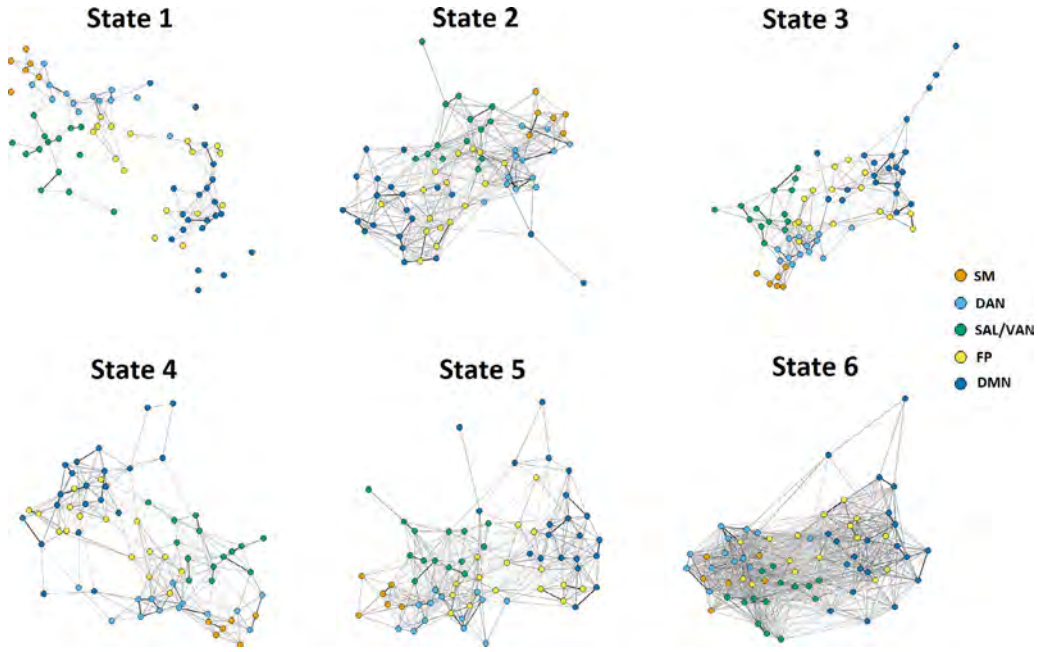

Fig. 5. Graph representations of the top 20% of positive correlations for all six states (overall across all states). Edge widths and color are proportional to correlation value (darker and wider edges represent higher positive correlations). Vertices are color-coded according to brain sub-network. Graphs are plotted using the *igraph* R package and the Fruchterman-Reingold layout (Fruchterman and Reingold, 1991), in which nodes that are more highly connected are placed near each other by the algorithm.

Table 3
Dwell times (represented by percentage of total time) for each state for participants with ADHD as compared to TD participants. *P*-values are generated from permutation testing.

	State 1	State 2	State 3	State 4	State 5	State 6
ADHD	7.09%	12.55%	8.60%	18.10%	15.05%	38.61%
TD	15.48%	14.50%	15.53%	13.17%	16.84%	24.50%
P-values	0.014	0.728	0.048	0.148	0.376	<0.001

of time in states 4 and 6, and a smaller percentage of time in states 1, 2, 3, and 5, as compared to TD children. The biggest differences in average dwell time between the two groups were for states 1, 3, and 6, which corresponded to the anticorrelated states and the hyperconnected state (Fig. 7, Table 3). Permutation testing revealed that children with ADHD spent significantly less time in states 1 (p =.014) and 3 (p =.048), and significantly more time in state 6 (p <0.001), than TD children. There was no statistically significant dwell time difference across groups for the other three states (Table 3).

3.4. State sojourn times

The sojourn time represents how long a participant spends in a state before transitioning to another state. Similar to dwell times, we conducted permutation testing and we found a significant difference in sojourn distributions between the two groups for state 3, the anticorrelated state with relatively strong positive correlations within and between the SM and DAN (p =.044), and state 6, the hyperconnected state (p =.002; Fig. 8). Specifically, we found that children with ADHD spent less time in the anticorrelated state (state 3) and more time in the hyperconnected state (state 6), before switching to another state compared with TD children. Group difference p-values for the remaining states were all p > 0.60.

3.5. State transition probabilities

Additionally, the two groups of participants differed in how likely they were to transition to each of the other states from their current state (Fig. 9). The participants with ADHD transitioned into state 6 (the hyperconnected state) from states 3 and 4 (two anticorrelated states) more often than the TD participants, as well as from state 1 (another anticorrelated state) into state 5 (a state with few anticorrelations). They additionally transitioned less often from state 6 (the hyperconnected state) into state 1 (the state with the strongest anticorrelations), as well as from state 4 (an anticorrelated state) into state 2 (a state with few anticorrelations).

3.6. Relationships with ADHD symptoms

Finally, we related dwell time, mean sojourn time, and maximum sojourn time of the states that showed significant group differences to symptom severity in the participants with ADHD. Specifically, we correlated inattentive and hyperactive symptoms with dwell time for states 1, 3 and 6, and both mean and maximum sojourn times for states 3 and 6. After FDR-correction for 14 comparisons, we did not observe any relationships between the HSMM-derived metrics and symptoms (all FDR-corrected p-values >.51).

4. Discussion

Differences in static FC between children with ADHD and TD children, on both the whole-brain scale and as related to specific sub-networks, have been reported (Cao et al., 2014; Gao et al., 2019; Henry and Cohen, 2019; Sutcubasi et al., 2020). However, specific regions are not consistent across studies (Cortese et al., 2020), indicating the need for other methods to distinguish ADHD from TD individuals. A small but emerging literature investigating dynamic FC in ADHD has observed differences in the temporal patterns of FC between ADHD and control participants (Abbas et al., 2019; Cai et al., 2018; de Lacy and Calhoun, 2019; Kaboodvand et al., 2020; Wang et al., 2018) and may thus pro-

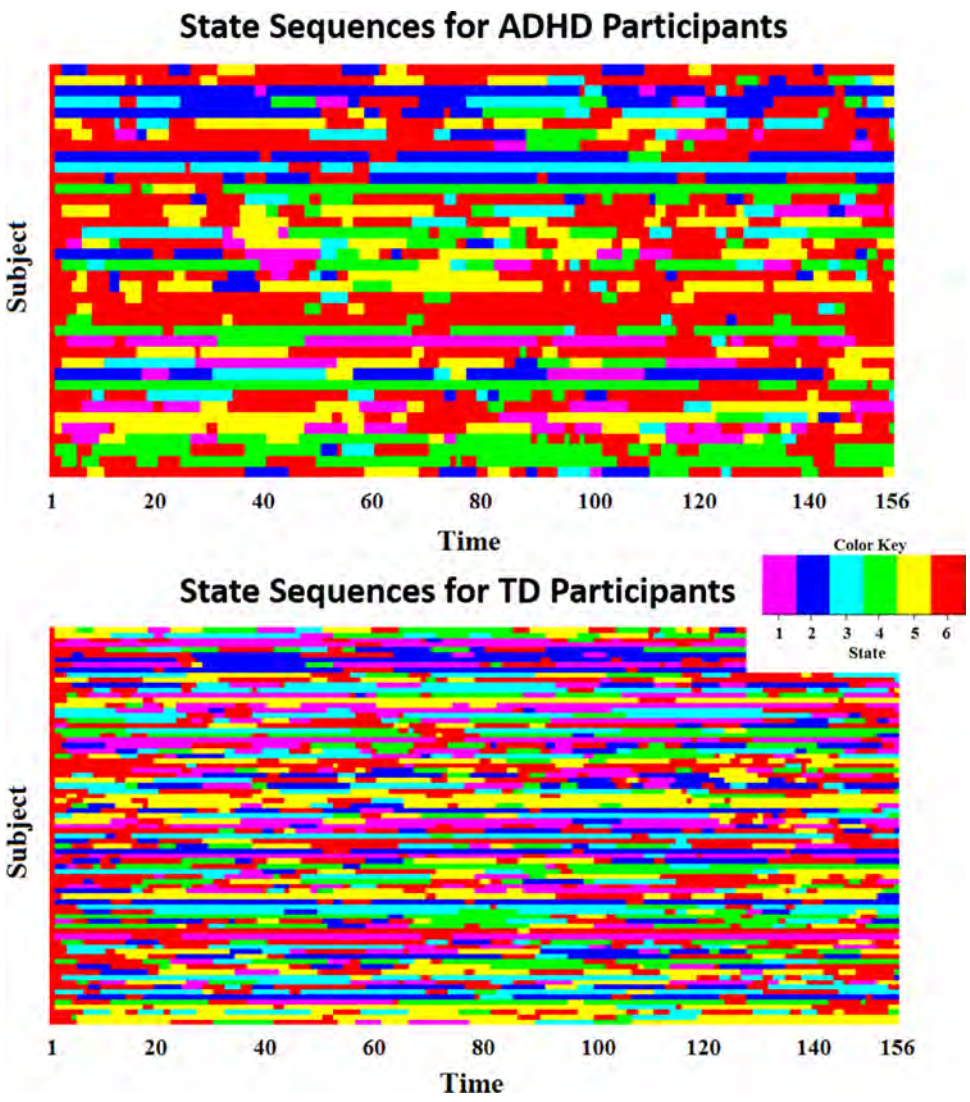

Fig. 6. (Top) State sequences across time observed for participants with ADHD. (Bottom) State sequences across time observed for TD participants. Note that 9 TD participants underwent shorter resting state scans (128 volumes, as compared to 156), thus their sequences end earlier in the plot.

vide insight beyond that which has been gained from static FC studies. Thus far, this research has largely used sliding window or instantaneous phase synchrony approaches. Here, we extend this literature by using an HSMM to obtain the most likely sequence of states for each participant in a maximum likelihood model-based manner. This method has advantages over the prior approaches in that the sojourn distribution is built directly into the model, and therefore, it is possible to better characterize additional aspects of dynamic FC, such as sojourn time distributions (Shappell et al., 2019). Thus, we were able to investigate whether children with ADHD differ from TD children in how long they spend in each state before transitioning to a different state. This feature of dynamic FC may be particularly relevant to ADHD given hypotheses that an inability to maintain states with reduced DMN connectivity may contribute to variability in attention and behavior (Sonuga-Barke and Castellanos, 2007).

We estimated six network states that children with ADHD and TD children transitioned in and out of during a resting state fMRI scan, as well as each participant's most probable sequence of states. This allowed us to quantify and compare the amount of time spent in each state, the probabilities of transitioning from one particular state to another, and the speed at which the participants switched out of states. We observed that children with ADHD spent less time in states characterized by anticorrelations between the DMN and task-relevant networks, particularly the SAL/VAN, as well as by strong positive correlations between the DAN and SM. Conversely, they spent more time in a globally hyperconnected state. This was the case when characterizing both dwell times (i.e., percent of time spent in each state) and sojourn distributions (i.e., number of consecutive timepoints in each state). Additionally, we observed that children with ADHD were less likely to transition into anticorrelated states and more likely to transition into hyperconnected states as compared to TD children.

Our finding that children with ADHD spent less time in multiple anticorrelated states (states 1 and 3), and were less likely to sustain an anticorrelated state (state 3), extends static FC literature that has demonstrated an overall reduction in anticorrelations between DMN and task-relevant network regions in ADHD, including attention-related networks such as the VAN (Kessler et al., 2014; Mills et al., 2018; Sripada et al., 2014; Sun et al., 2012). It additionally helps to resolve recent findings in contrast to this older literature that has observed a lack of static FC differences in DMN functioning in ADHD (Cortese et al., 2020; Dajani et al., 2019; de Lacy and Calhoun, 2019). While theories have been proposed stating that children with ADHD may have trouble maintaining sustained, on-task attention due to DMN intrusions into task-related processing (Sonuga-Barke and Castellanos, 2007; Weissman et al., 2006), current evidence for these theories is limited to activation analyses (i.e., findings that reduced deactivation of DMN brain regions during cognitive tasks is related to poorer task performance) (Fassbender et al., 2009; Helps et al., 2010) and static FC analyses (i.e., findings of reduced static

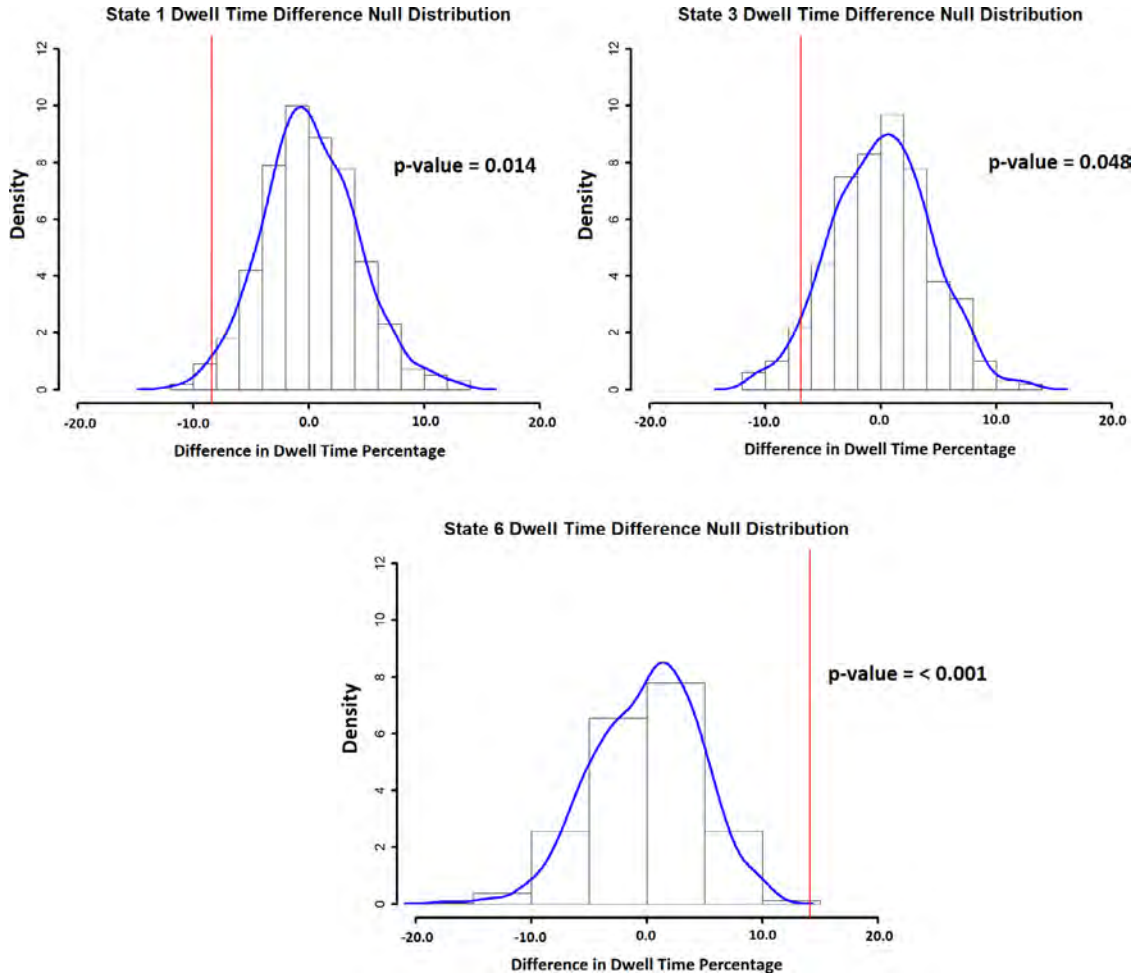

Fig. 7. Permutation test results obtained from permuting ADHD/TD group labels 500 times and computing the difference in state 1, 3, and 6 dwell times between the two groups for each of these 500 sets. The vertical line in each plot depicts where the observed group difference in dwell time fell with respect to the null distribution, with group differences to the left of the null distribution indicating a greater dwell time for TD children and differences to the right of the null distribution indicating a greater dwell time for children with ADHD.

FC anticorrelations during rest) (Mills et al., 2018). Dynamic FC analyses such as those implemented here are better suited to directly test the dynamic aspect of these theories, namely that attention is a cyclical process with periods of waxing and waning attention. Specifically, the current findings provide novel evidence that children with ADHD are less likely to enter into or remain in DMN anticorrelated states as compared to TD children. To more directly test the hypothesis that reduced time in an anticorrelated state is a mechanism for inattention in ADHD, future studies probing dynamic FC during task performance and using directed connectivity to assess the impact of DMN on task-relevant networks are necessary.

States 1 and 3 additionally had strong positive correlations within and between pairs of task-relevant networks, the SM and DAN in particular. Using static FC methods, reduced FC of the DAN (Cubillo et al., 2010; Kessler et al., 2014; McCarthy et al., 2013; Zhu et al., 2008) and within primary somatosensory cortices (McLeod et al., 2014) have been found in resting state fMRI studies of children and adults with ADHD. Thus, the reduced time and number of transitions into a state with strong positive SM-DAN connections, in addition to indicating a reduced ability to sustain attention, may imply a mechanism for the poorer motor functioning observed in children with ADHD (Cole et al., 2008; Gilbert et al., 2011; 2019; MacNeil et al., 2011; Mostofsky et al., 2003).

We additionally found that children with ADHD were more likely to transition into a hyperconnected state (state 6) characterized by high global and local efficiency and low modularity as compared to TD children, and that they tended to remain in this state longer after transitioning into it. This state was hyperconnected both within and across sub-networks without a strong bias for segregation across sub-networks. This result clarifies static FC findings of increased global connectivity and/or lack of segregation between sub-networks in resting state FC in ADHD (Kessler et al., 2014; Qian et al., 2019; Sörös et al., 2019). Specifically, our dynamic FC analysis provides evidence that the static FC findings demonstrating a general increase in hyperconnectivity in ADHD may be due to reduced ability of individuals with ADHD to sustain anticorrelated states and transition out of hyperconnected states. A more modular, specialized brain network organization emerges throughout development and is associated with increased executive functioning (Baum et al., 2017). Thus, an increased tendency to be in a less specialized, hyperconnected state may indicate support for the maturational lag hypothesis in ADHD (El-Sayed et al., 2003; Shaw et al., 2007) and may additionally underlie the executive functioning deficits commonly observed in ADHD. Notably, prior studies using graph theory with static FC data to characterize network organization have found increased local efficiency in ADHD (consistent with our results of children with ADHD spending more time in a highly locally efficient state), but decreased global efficiency (inconsistent with our results of this state also being high in global efficiency, although significant differences in global efficiency are limited to adults with ADHD and may thus be due to developmental factors) (Lin et al., 2014; Wang et al., 2009). This highlights the additional information that can be gained by taking dynamics into

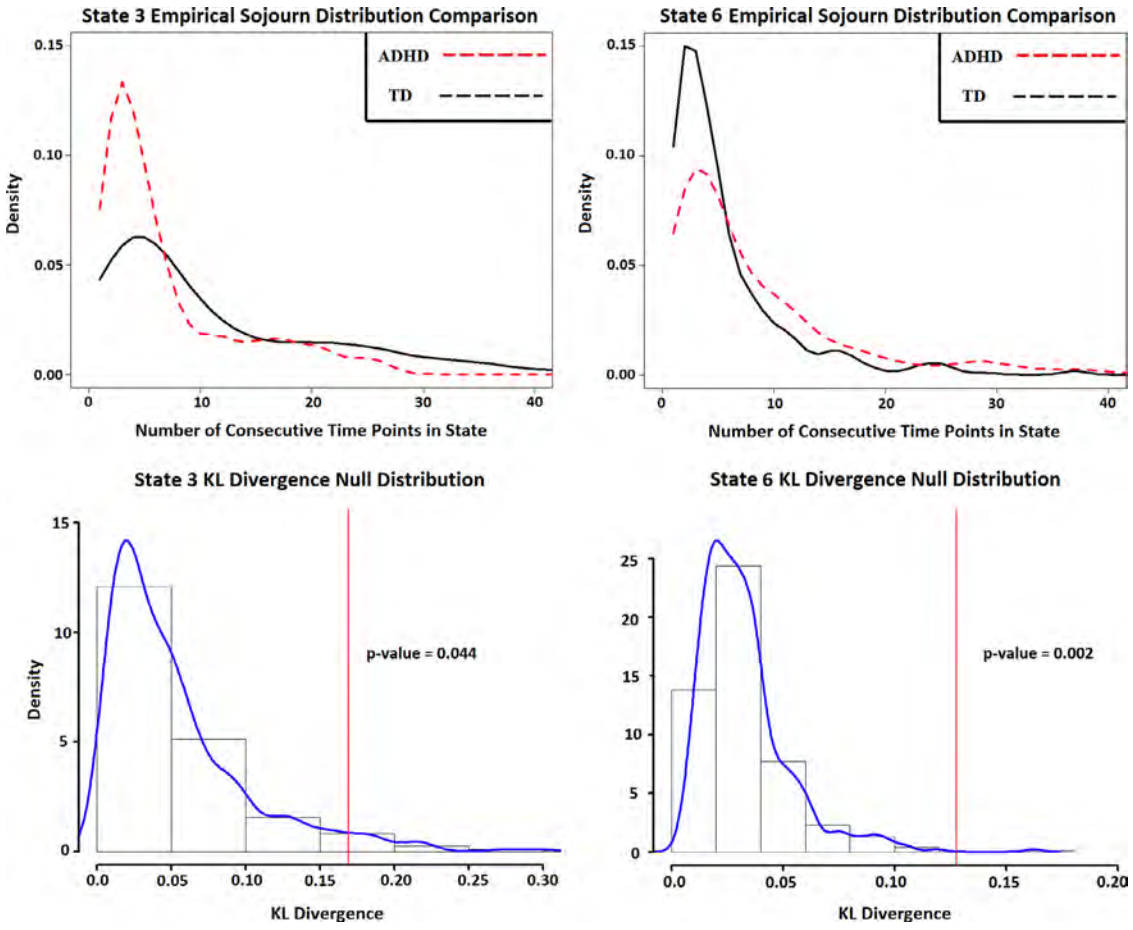

Fig. 8. (Top) Estimated empirical sojourn distributions for states 3 and 6 for the ADHD and TD groups, indicating that children with ADHD spend less time in state 3 and more time in state 6 than TD children before switching to another state. (Bottom) Permutation test results obtained from permuting the ADHD/TD group labels 500 times and calculating the Kullback-Leibler (KL) divergence (a measure of how similar the two distributions are) between the states for each of those 500 sets. The vertical line in each plot depicts where the observed KL divergence fell with respect to the null distribution.

account, namely that FC patterns change throughout the course of a resting state scan, and it is the dynamics that differ between children with ADHD and TD children as opposed to the functional connectivity patterns of the states in general. We report support for this claim in our *Supplementary Material*, in which we demonstrated that the FC states are similar across the ADHD and TD groups even when estimating states for each group separately. Future longitudinal investigations can more directly assess whether our findings related to the hyperconnected state support the maturational lag hypothesis of ADHD. Further, relating dynamic FC characteristics to behavioral measures of executive functioning would directly assess whether dysfunction in dynamic FC underlies executive functioning deficits in ADHD.

In addition to characterizing state patterns and transitions in our participants, we examined whether characteristics of the state dynamics were related to symptoms in the participants with ADHD. We did not find that ADHD symptoms were related to dwell time, mean sojourn time, or maximum sojourn time of any of the states that showed significant group differences (states 1, 3, and 6). This could be due to a few reasons. First, it is possible that the state dynamics reflect categorical group differences and thus there is not a relationship between symptom severity and HSMM metrics. Second, for the sojourn distribution parameters in particular, we could not estimate the entire distribution on the level of single participants, thus we related summary measures (mean, maximum) that may be less sensitive to individual differences than the full distributions. Finally, we have a relatively small sample of participants with ADHD (n = 38), thus we may not have had the power to observe significant relationships with the dynamic state metrics given the underlying effect size. Future research should further investigate the relationship between participant characteristics and HSMM metrics in a larger sample with more data per participant to differentiate between these possibilities.

Together, our findings extend existing studies implementing dynamic FC in ADHD, which support the idea that whole-brain dynamic FC measures discriminate between ADHD and TD participants (Wang et al., 2018), particularly as related to DMN inter-network connections. Reduced dynamics of the DMN in general have been observed in ADHD (de Lacy and Calhoun, 2019), as have DMN–sensory network interactions (Wang et al., 2018) and DMN–higher-order task-relevant network interactions (including regions related to cognitive control and attention) (Abbas et al., 2019). Conversely, however, other studies have observed increased FC dynamics between the DMN and task-relevant networks in ADHD (Cai et al., 2018; Kaboodvand et al., 2020). While we did not focus specifically on the DMN in our analyses, we observed that children with ADHD were less likely to enter into or sustain states characterized by DMN-related anticorrelations. Notably, we also observed that these anticorrelated states were characterized by increased connectivity between task-relevant networks known to be dysfunctional in ADHD, namely the DAN and SM. Thus, our focus on whole-brain states instead of focusing on specific networks expands existing findings to provide a fuller picture of alterations in dynamic FC in ADHD. To fully understand how these network alterations underlie cognitive deficits observed in ADHD (i.e., poorer motor function, attention, and executive function-

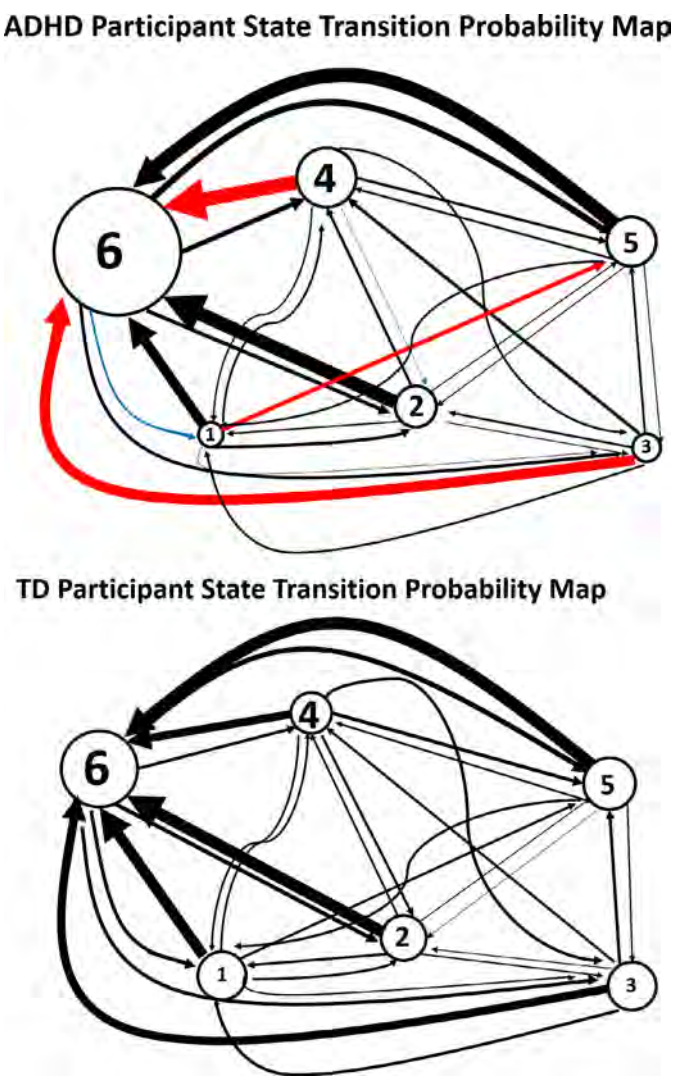

Fig. 9. A visual representation of the conditional transition probabilities between states, as well as the state dwell times. Edge widths are proportional to the conditional transitional probabilities between states, with thicker edges representing a higher probability. State node sizes are proportional to the dwell time of each state. We highlighted the five largest conditional probability differences between the two groups with red and blue arrows. Red arrows in the top figure for ADHD participants indicate a relatively high transition probability as compared to the TD participants (greater than a 7.5% chance of transitioning increase). Blue arrows indicate a relatively low transition probability in the ADHD group as compared to the TD group (greater than a 7.5% chance of transitioning decrease).

ing), conducting similar analyses during cognitive task performance is needed.

Importantly, though we excluded participants with ADHD from the larger study from which our sample was pulled, the current sample did not differ from the larger sample in terms of any of the diagnostic or clinical criteria on which we compared the groups (age, sex, socioeconomic status, IQ, ADHD symptomatology, comorbidities, or treatment status). Further, it is important to note that we chose to include a sample of participants with ADHD that had other comorbid disorders. It has been reported that the number of youth with ADHD with at least one comorbid disorder is as high as 73% (Taurines et al., 2010), thus we chose to prioritize a more representative sample of children with ADHD over a "pure" ADHD sample, which would be less generalizable. For the same reason, we did not exclude participants with ADHD who were taking stimulant medication, the recommended first-line treatment for ADHD (Austerman, 2015), or children taking medication to treat their comorbidities (SSRIs, antipsychotics). While this decision limits our ability to conclude that the dynamic FC differences we observed in our ADHD group is specific to ADHD, the ability to generalize to a representative population is a strength of the study. Future research in a larger sample with a balance of participants with and without comorbidities would be able to tease apart dynamic FC differences due specifically to ADHD versus due to ADHD-related pathology in general.

Though we chose not to match our groups on in-scanner motion (mean FD) due to evidence that in-scanner motion is a characteristic of ADHD (Couvy-Duchesne et al., 2016), we took rigorous steps to ensure that mean FD did not drive our results. Our data processing, chosen because of its ability to sufficiently reduce spurious effects of motion (Ciric et al., 2017; Parkes et al., 2018), greatly reduced motion-related artifacts in our data according to quality control criteria (see *Supplementary Material*) (Ciric et al., 2017). To ensure that after processing motion did not have a large impact on our findings, we correlated mean FD with the HSMM metrics across our states and found that only one HSMM metric for a single state was related to motion (the dwell time of state 6; see *Supplementary Material*). This is not surprising given that state 6 was more often observed during high motion timepoints than the other states, indicating that it may be a functional connectivity pattern that reflects increased in-scanner motion. If so, it is not surprising that participants with ADHD, who had higher motion than TD participants, spent more time in this state and were more likely to transition into this state from other states. Further research probing whether this state is a neural feature of ADHD or an artifact of motion is needed. Importantly, despite this potential confound regarding state 6, states 1 and 3, which are both anticorrelated states, were not related to motion. Thus, our finding that participants with ADHD spent less time in and were more likely to transition out of anticorrelated states as compared to TD participants is not confounded by the difference in mean FD across our groups.

Finally, we chose to fit one set of states for all participants, despite the sample being predominantly TD (68%). We believe this is appropriate given that the HSMM does not simply average across all participants, but instead estimates different states that best fit and capture both the similarities and differences in the data. We found that six states properly fit the data, allowing for variability between the states entered by TD children and children with ADHD. Critically, as reported in the *Supplementary Material*, when fitting states for each group separately results were strikingly similar to the states estimated from the full sample, justifying our decision to combine across groups to maximize the data going into the model. In the future, it would be useful to define participant-specific states to allow for as much individuality as possible. In order to do so, however, random effects would need to be incorporated into the HSMM. A mixed-effects HSMM framework will be developed in future work to enable individual state-fitting, as well as to enable covariates such as sex, age, or behavior to be included as fixed effects directly in the HSMM. Lastly, it should be noted as a limitation that the study was not pre-registered.

4.1. Conclusions

To conclude, we investigated the dynamic mechanisms of brain network dysfunction in ADHD. We found that children with ADHD spent less total time in and switched more quickly out of anticorrelated states characterized by a greater number of negative correlations between the DMN and other sub-networks, particularly the SAL/VAN, as well as by strong positive correlations between the DAN and SM. Additionally, we found that children with ADHD spent more time in a hyperconnected state characterized by high global and local efficiency and low modularity as compared to TD children. These results demonstrate the utility of the HSMM model when investigating network connectivity dynamics. Importantly, they may indicate a mechanism for the behavioral symptoms and cognitive deficits commonly observed in children with ADHD,

particularly as related to attention, motor functioning, and executive function. To further probe this potential mechanism, future research should relate characteristics of dynamic FC to cognitive performance, as well as assess dynamic FC during cognitive tasks. Finally, longitudinal studies are needed to investigate the potential of a maturational delay of dynamic FC in children with ADHD.

Data and code availability statement

Data was collected as part of an ongoing National Institutes of Health (NIH) grant and will be made available after completion of the study as per NIH data sharing requirements. The HSMM code is available upon request. In the future, it will be developed into a publicly available toolbox.

Declarations of Competing Interest

SHM has a US patent (Patent No: US10,410,041 B2). All other authors report no biomedical financial interests or potential conflicts of interest.

Funding

This work was supported by National Institutes of Health [grant numbers R01MH085328 and R01MH078160 to SHM, R00MH102349 to JRC, R01EB016061 and R01EB026549 to MAL, K23MH101322 to KSR, T32DA050560 to KAD, and 5P41EB015909 to JJP]; and Johns Hopkins University School of Medicine Institute for Clinical and Translational Research NIH/National Center for Research Resources Clinical and Translational Science Award program [grant number UL1TR000424 to KSR].

Supplementary material

Supplementary material associated with this article can be found, in the online version, at 10.1016/j.neuroimage.2021.117753

Credit authorship contribution statement

Heather M. Shappell: Conceptualization, Methodology, Software, Formal analysis, Visualization, Writing - original draft, Writing - review & editing. **Kelly A. Duffy:** Data curation, Software, Formal analysis, Writing - original draft, Writing - review & editing. **Keri S. Rosch:** Funding acquisition, Investigation, Data curation, Writing - review & editing. **James J. Pekar:** Supervision, Writing - review & editing. **Stewart H. Mostofsky:** Funding acquisition, Resources, Project administration, Investigation, Writing - review & editing. **Martin A. Lindquist:** Conceptualization, Supervision, Project administration, Methodology, Visualization, Writing - review & editing. **Jessica R. Cohen:** Conceptualization, Supervision, Project administration, Data curation, Methodology, Writing - original draft, Writing - review & editing.

References

Abbas, A., Bassil, Y., Keilholz, S., 2019. Quasi-periodic patterns of brain activity in individuals with attention-deficit/hyperactivity disorder. NeuroImage: Clinical 21, 101653.
Abraham, A., Pedregosa, F., Eickenberg, M., Gervais, P., Mueller, A., Kossaifi, J., et al., 2014. Machine learning for neuroimaging with scikit-learn. Front. Neuroinform. 8.
Austerman, J., 2015. ADHD and behavioral disorders: assessment, management, and an update from DSM-5. Cleveland Clin. J. Med. 82 (11 suppl 1), S2–S7.
Avants, B., Epstein, C., Grossman, M., Gee, J., 2008. Symmetric diffeomorphic image registration with cross-correlation: evaluating automated labeling of elderly and neurodegenerative brain. Med. Image Anal. 12 (1), 26–41.
Baum, G.L., Ciric, R., Roalf, D.R., Betzel, R.F., Moore, T.M., Shinohara, R.T., Kahn, A.E., et al., 2017. Modular segregation of structural brain networks supports the development of executive function in youth. Curr. Biol. 27 (11), 1561–1572.
Cai, W., Chen, T., Szegletes, L., Supekar, K., Menon, V., 2018. Aberrant time-varying cross-network interactions in children with attention-deficit/hyperactivity disorder and the relation to attention deficits. Biol. Psychiatry: CNNI 3 (3), 263–273.
Calhoun, V.D., Miller, R., Pearlson, G., Adalı, T., 2014. The chronnectome: time-varying connectivity networks as the next frontier in fMRI data discovery. Neuron 84 (2), 262–274.
Cao, M., Shu, N., Cao, Q., Wang, Y., He, Y., 2014. Imaging functional and structural brain connectomics in attention-deficit/hyperactivity disorder. Mol. Neurobiol. 50 (3), 1111–1123.
Castellanos, F.X., Aoki, Y., 2016. Intrinsic functional connectivity in attention-deficit/hyperactivity disorder: a science in development. Biol. Psychiatry: CNNI 1 (3), 253–261.
Castellanos, F.X., Kelly, C., Milham, M.P., 2009. The restless brain: attention-deficit hyperactivity disorder, resting-state functional connectivity, and intrasubject variability. Can. J. Psychiatry 54 (10), 665–672.
Castellanos, F.X., Proal, E., 2012. Large-scale brain systems in ADHD: beyond the prefrontal–striatal model. Trends Cognit. Sci. 16 (1), 17–26.
Castellanos, F.X., Sonuga-Barke, E.J., Scheres, A., Di Martino, A., Hyde, C., Walters, J.R., 2005. Varieties of attention-deficit/hyperactivity disorder-related intra-individual variability. Biol. Psychiatry 57 (11), 1416–1423.
Ciric, R., Wolf, D.H., Power, J.D., Roalf, D.R., Baum, G.L., Ruparel, K., Shinohara, R.T., Elliott, M.A., Eickhoff, S.B., Davatzikos, C., et al., 2017. Benchmarking of participant-level confound regression strategies for the control of motion artifact in studies of functional connectivity. NeuroImage 154, 174–187.
Cohen, J.R., 2018. The behavioral and cognitive relevance of time-varying, dynamic changes in functional connectivity. NeuroImage 180, 515–525.
Cole, W., Mostofsky, S.H., Larson, J.G., Denckla, M.B., Mahone, E.M., 2008. Age-related changes in motor subtle signs among girls and boys with ADHD. Neurology 71 (19), 1514–1520.
Conners, C., 2002. Conners' Rating Scales, Revised. Multi-Health Systems Inc, Toronto.
Conners, C., 2008. Conners' 3. Multi-Health Systems Inc, North Tonawanda, NY.
Cortese, S., Aoki, Y.Y., Itahashi, T., Castellanos, F.X., Eickhoff, S.B., 2020. Systematic review and meta-analysis: resting state functional magnetic resonance imaging studies of attention-deficit/hyperactivity disorder. J. Am. Acad. Child Adolesc. Psychiatry e-pub ahead of print (doi:10.1016/j.jaac.2020.08.014).
Couvy-Duchesne, B., Ebejer, J.L., Gillespie, N.A., Duffy, D.L., Hickie, I.B., Thompson, P.M., et al., 2016. Head motion and inattention/hyperactivity share common genetic influences: implications for fMRI studies of ADHD. PLoS One 11 (1), e0146271.
Cox, R.W., 1996. AFNI: software for analysis and visualization of functional magnetic resonance neuroimages. Comput. Biomed. Res. 29 (3), 162–173.
Cubillo, A., Halari, R., Ecker, C., Giampietro, V., Taylor, E., Rubia, K., 2010. Reduced activation and inter-regional functional connectivity of fronto-striatal networks in adults with childhood attention-deficit hyperactivity disorder (ADHD) and persisting symptoms during tasks of motor inhibition and cognitive switching. J. Psychiatr. Res. 44 (10), 629–639.
Dajani, D.R., Burrows, C.A., Odriozola, P., Baez, A., Nebel, M.B., Mostofsky, S.H., Uddin, L.Q., 2019. Investigating functional brain network integrity using a traditional and novel categorical scheme for neurodevelopmental disorders. NeuroImage: Clinical 21, 101678.
Dempster, A.P., Laird, N.M., Rubin, D.B., 1977. Maximum likelihood from incomplete data via the EM algorithm. J. R. Stat. Soc. Series B (Methodological) 1–38.
Di Martino, A., Ghaffari, M., Curchack, J., Reiss, P., Hyde, C., Vannucci, M., et al., 2008. Decomposing intra-subject variability in children with attention-deficit/hyperactivity disorder. Biol. Psychiatry 64 (7), 607–614.
DuPaul, G.J., Power, T.J., Anastopoulos, A.D., Reid, R., 1998. ADHD Rating Scale-IV: Checklists, Norms, and Clinical Interpretation.. Guilford Press.
El-Sayed, E., Larsson, J.-O., Persson, H., Santosh, P., Rydelius, P.-A., 2003. Maturational lag hypothesis of attention deficit hyperactivity disorder: an update. Acta Paediatr. 92 (7), 776–784.
Esteban, O., Markiewicz, C.J., Blair, R.W., Moodie, C.A., Isik, A.I., Erramuzpe, A., et al., 2019. fMRIPrep: a robust preprocessing pipeline for functional MRI. Nat. Methods 16 (1), 111–116.
Fair, D.A., Posner, J., Nagel, B.J., Bathula, D., Dias, T.G.C., Mills, K.L., et al., 2010. Atypical default network connectivity in youth with attention-deficit/hyperactivity disorder. Biol. Psychiatry 68 (12), 1084–1091.
Fassbender, C., Zhang, H., Buzy, W.M., Cortes, C.R., Mizuiri, D., Beckett, L., et al., 2009. A lack of default network suppression is linked to increased distractibility in ADHD. Brain Res. 1273, 114–128.
Fonov, V., Evans, A., McKinstry, R., Almli, C., Collins, D., 2009. Unbiased nonlinear average age-appropriate brain templates from birth to adulthood. NeuroImage 47, S102.
Forney, G.D., 1973. The viterbi algorithm. Proc. IEEE 61 (3), 268–278.
Fruchterman, T.M., Reingold, E.M., 1991. Graph drawing by force-directed placement. Software 21 (11), 1129–1164.
Gao, Y., Shuai, D., Bu, X., Hu, X., Tang, S., Zhang, L., Li, H., Hu, X., Lu, L., Gong, Q., et al., 2019. Impairments of large-scale functional networks in attention-deficit/hyperactivity disorder: a meta-analysis of resting-state functional connectivity. Psychol. Med. 49 (15), 2475–2485.
Gilbert, D., Isaacs, K., Augusta, M., Macneil, L., Mostofsky, S.H., 2011. Motor cortex inhibition: a marker of ADHD behavior and motor development in children. Neurology 76 (7), 615–621.
Gilbert, D.L., Huddleston, D.A., Wu, S.W., Pedapati, E.V., Horn, P.S., Hirabayashi, K., et al., 2019. Motor cortex inhibition and modulation in children with ADHD. Neurology 93 (6), e599–e610.
Gorgolewski, K., Burns, C.D., Madison, C., Clark, D., Halchenko, Y.O., Waskom, M.L., et al., 2011. Nipype: a flexible, lightweight and extensible neuroimaging data processing framework in Python. Front. Neuroinform. 5, 13.
Gorgolewski, K. J., Esteban, O., Ellis, D. G., Notter, M. P., Ziegler, E., Johnson, H., et al., 2017. Nipype: a flexible, lightweight and extensible neuroimaging data processing framework in python. 0.13.1. Zenodo. doi:10.5281/zenodo.581704.

Greve, D.N., Fischl, B., 2009. Accurate and robust brain image alignment using boundary-based registration. NeuroImage 48 (1), 63–72.
Helps, S.K., Broyd, S.J., James, C.J., Karl, A., Chen, W., Sonuga-Barke, E.J., 2010. Altered spontaneous low frequency brain activity in attention deficit/hyperactivity disorder. Brain Res. 1322, 134–143.
Henry, T.R., Cohen, J.R., 2019. Dysfunctional brain network organization in neurodevelopmental disorders. In: Connectomics. Elsevier, pp. 83–100.
Hollingshead, A.d.B., 1975. Four Factor Index of Social Status. Yale University, Dept. of Sociology, New Haven, Conn..
Hutchison, R.M., Womelsdorf, T., Allen, E.A., Bandettini, P.A., Calhoun, V.D., Corbetta, M., et al., 2013. Dynamic functional connectivity: promise, issues, and interpretations. NeuroImage 80, 360–378.
Jenkinson, M., Bannister, P., Brady, M., Smith, S., 2002. Improved optimization for the robust and accurate linear registration and motion correction of brain images. NeuroImage 17 (2), 825–841.
Kaboodvand, N., Iravani, B., Fransson, P., 2020. Dynamic synergetic configurations of resting-state networks in ADHD. NeuroImage 207, 116347.
Karalunas, S.L., Geurts, H.M., Konrad, K., Bender, S., Nigg, J.T., 2014. Reaction time variability in ADHD and autism spectrum disorders: Measurement and mechanisms of a proposed trans-diagnostic phenotype. J. Child Psychol. Psychiatry 55 (6), 685–710.
Karalunas, S.L., Huang-Pollock, C.L., Nigg, J.T., 2013. Is reaction time variability in ADHD mainly at low frequencies? J. Child Psychol. Psychiatry 54 (5), 536–544.
Kaufman, J., Birmaher, B., Brent, D., Rao, U., Flynn, C., Moreci, P., et al., 1997. Schedule for affective disorders and schizophrenia for school-age children-present and lifetime version (K-SADS-PL): initial reliability and validity data. J. Am. Acad. Child Adolesc. Psychiatry 36 (7), 980–988.
Kessler, D., Angstadt, M., Welsh, R.C., Sripada, C., 2014. Modality-spanning deficits in attention-deficit/hyperactivity disorder in functional networks, gray matter, and white matter. J. Neurosci. 34 (50), 16555–16566.
Klein, A., Ghosh, S.S., Bao, F.S., Giard, J., Hme, Y., Stavsky, E., et al., 2017. Mindboggling morphometry of human brains. PLoS Comput. Biol. 13 (2), e1005350.
Kofler, M.J., Rapport, M.D., Sarver, D.E., Raiker, J.S., Orban, S.A., Friedman, L.M., et al., 2013. Reaction time variability in ADHD: a meta-analytic review of 319 studies. Clin. Psychol. Rev. 33 (6), 795–811.
Kucyi, A., Tambini, A., Sadaghiani, S., Keilholz, S., Cohen, J.R., 2018. Spontaneous cognitive processes and the behavioral validation of time-varying brain connectivity. Netw. Neurosci. 2 (4), 397–417.
Dale, A.M., Fischl, B., Sereno, M.I., 1999. Cortical surface-based analysis. NeuroImage 9 (2), 179–194.
de Lacy, N., Calhoun, V.D., 2019. Dynamic connectivity and the effects of maturation in youth with attention deficit hyperactivity disorder. Netw. Neurosci. 3 (1), 195–216.
Latora, V., Marchiori, M., 2001. Efficient behavior of small-world networks. Phys. Rev. Lett. 87 (19), 198701.
Lin, P., Sun, J., Yu, G., Wu, Y., Yang, Y., Liang, M., et al., 2014. Global and local brain network reorganization in attention-deficit/hyperactivity disorder. Brain Imaging Behav. 8 (4), 558–569.
Lurie, D.J., Kessler, D., Bassett, D.S., Betzel, R.F., Breakspear, M., Kheilholz, S., Kucyi, A., Ligeois, R., Lindquist, M.A., McIntosh, A.R., et al., 2020. Questions and controversies in the study of time-varying functional connectivity in resting fMRI. Netw. Neurosci. 4 (1), 30–69.
MacNeil, L., Xavier, P., Garvey, M., Gilbert, D., Ranta, M., Denckla, M.B., et al., 2011. Quantifying excessive mirror overflow in children with attention-deficit/hyperactivity disorder. Neurology 76 (7), 622–628.
McCarthy, H., Skokauskas, N., Mulligan, A., Donohoe, G., Mullins, D., Kelly, J., et al., 2013. Attention network hypoconnectivity with default and affective network hyperconnectivity in adults diagnosed with attention-deficit/hyperactivity disorder in childhood. JAMA Psychiatry 70 (12), 1329–1337.
McLeod, K.R., Langevin, L.M., Goodyear, B.G., Dewey, D., 2014. Functional connectivity of neural motor networks is disrupted in children with developmental coordination disorder and attention-deficit/hyperactivity disorder. NeuroImage 4, 566–575.
Mills, B.D., Miranda-Dominguez, O., Mills, K.L., Earl, E., Cordova, M., Painter, J., et al., 2018. ADHD and attentional control: Impaired segregation of task positive and task negative brain networks. Netw. Neurosci. 2 (02), 200–217.
Mostofsky, S.H., Newschaffer, C.J., Denckla, M.B., 2003. Overflow movements predict impaired response inhibition in children with ADHD. Perceptual Motor Skills 97 (3_suppl), 1315–1331.
Newman, M.E.J., 2004. Fast algorithm for detecting community structure in networks. Phys. Rev. E 69 (6), 066133.
O'Connell, J., Højsgaard, S., et al., 2011. Hidden semi Markov models for multiple observation sequences: the MHSMM package for R. J. Stat. Softw. 39 (4), 1–22.
Parkes, L., Fulcher, B., Ycel, M., Fornito, A., 2018. An evaluation of the efficacy, reliability, and sensitivity of motion correction strategies for resting-state functional MRI. NeuroImage 171, 415–436.
Power, J.D., Mitra, A., Laumann, T.O., Snyder, A.Z., Schlaggar, B.L., Petersen, S.E., 2014. Methods to detect, characterize, and remove motion artifact in resting state fMRI. NeuroImage 84, 320–341.
Qian, X., Castellanos, F.X., Uddin, L.Q., Loo, B.R.Y., Liu, S., Koh, H.L., et al., 2019. Large-scale brain functional network topology disruptions underlie symptom heterogeneity in children with attention-deficit/hyperactivity disorder. NeuroImage: Clinical 21, 101600.
Reich, W., Welner, Z., Herjanic, B., 1997. Diagnostic Interview for Children and Adolescents-IV. Multi-Health System, North Towanda Falls, NY.
Rubinov, M., Sporns, O., 2010. Complex network measures of brain connectivity: uses and interpretations. NeuroImage 52 (3), 1059–1069.
Schaefer, A., Kong, R., Gordon, E.M., Laumann, T.O., Zuo, X.-N., Holmes, A.J., et al., 2018. Local-global parcellation of the human cerebral cortex from intrinsic functional connectivity MRI. Cereb. Cortex 28 (9), 3095–3114.
Shappell, H., Caffo, B.S., Pekar, J.J., Lindquist, M.A., 2019. Improved state change estimation in dynamic functional connectivity using hidden semi-Markov models. NeuroImage 191, 243–257.
Shaw, P., Eckstrand, K., Sharp, W., Blumenthal, J., Lerch, J., Greenstein, D., et al., 2007. Attention-deficit/hyperactivity disorder is characterized by a delay in cortical maturation. Proc. Natl. Acad. Sci. 104 (49), 19649–19654.
Sonuga-Barke, E.J., Castellanos, F.X., 2007. Spontaneous attentional fluctuations in impaired states and pathological conditions: a neurobiological hypothesis. Neurosci. Biobehav. Rev. 31 (7), 977–986.
Sörös, P., Hoxhaj, E., Borel, P., Sadohara, C., Feige, B., Matthies, S., et al., 2019. Hyperactivity/restlessness is associated with increased functional connectivity in adults with ADHD: a dimensional analysis of resting state fMRI. BMC Psychiatry 19 (1), 43.
Sripada, C., Kessler, D., Fang, Y., Welsh, R.C., Prem Kumar, K., Angstadt, M., 2014. Disrupted network architecture of the resting brain in attention-deficit/hyperactivity disorder. Hum. Brain Map. 35 (9), 4693–4705.
Sun, L., Cao, Q., Long, X., Sui, M., Cao, X., Zhu, C., et al., 2012. Abnormal functional connectivity between the anterior cingulate and the default mode network in drug-naive boys with attention deficit hyperactivity disorder. Psychiatry Res. 201 (2), 120–127.
Sutcubasi, B., Metin, B., Kurban, M.K., Metin, Z.E., Beser, B., Sonuga-Barke, E., 2020. Resting-state network dysconnectivity in adhd: a system-neuroscience-based meta–analysis. World J. Biol. Psychiatry 21 (9), 662–672.
Taurines, R., Schmitt, J., Renner, T., Conner, A.C., Warnke, A., Romanos, M., 2010. Developmental comorbidity in attention-deficit/hyperactivity disorder. ADHD Attention Deficit Hyperact. Disord. 2 (4), 267–289.
Tustison, N.J., Avants, B.B., Cook, P.A., Zheng, Y., Egan, A., Yushkevich, P.A., et al., 2010. N4ITK: improved N3 bias correction. IEEE Trans. Med. Imaging 29 (6), 1310–1320.
Vaurio, R.G., Simmonds, D.J., Mostofsky, S.H., 2009. Increased intra-individual reaction time variability in attention-deficit/hyperactivity disorder across response inhibition tasks with different cognitive demands. Neuropsychologia 47 (12), 2389–2396.
Wang, L., Zhu, C., He, Y., Zang, Y., Cao, Q., Zhang, H., et al., 2009. Altered small-world brain functional networks in children with attention-deficit/hyperactivity disorder. Hum. Brain Map. 30 (2), 638–649.
Wang, X.-H., Jiao, Y., Li, L., 2018. Identifying individuals with attention deficit hyperactivity disorder based on temporal variability of dynamic functional connectivity. Sci. Rep. 8 (1), 11789.
Wechsler, D., 2003. Wechsler Individual Achievement Test, (second ed.) Psychological Corporation, San Antonio, TX.
Wechsler, D., 2003. Wechsler Intelligence Scale for Children. Psychological Corporation, San Antonio, TX.
Wechsler, D., 2009. Wechsler Intelligence Scale for Children, (third ed.) Pearson, San Antonio, TX.
Wechsler, D., 2014. Wechsler Intelligence Scale for Children. Pearson, Bloomington, MN.
Weissman, D.H., Roberts, K., Visscher, K., Woldorff, M., 2006. The neural bases of momentary lapses in attention. Nat. Neurosci. 9 (7), 971.
Yeo, B.T.T., Krienen, F.M., Sepulcre, J., Sabuncu, M.R., Lashkari, D., Hollinshead, M., et al., 2011. The organization of the human cerebral cortex estimated by intrinsic functional connectivity. J. Neurophysiol. 106 (3), 1125–1165.
Zhang, Y., Brady, M., Smith, S., 2001. Segmentation of brain MR images through a hidden Markov random field model and the expectation-maximization algorithm. IEEE Trans. Med. Imaging 20 (1), 45–57.
Zhu, C.-Z., Zang, Y.-F., Cao, Q.-J., Yan, C.-G., He, Y., Jiang, T.-Z., et al., 2008. Fisher discriminative analysis of resting-state brain function for attention-deficit/hyperactivity disorder. NeuroImage 40 (1), 110–120.